

Aromatic admixture impact on *n*-alkane hydrocracking over Pt/HUSY

Bernardo Alves Canudo

Supervisors: Prof. Dr. Pedro S. F. Mendes¹, Nebojsa Korica²

¹ Chemical Engineering Department, Instituto Superior Técnico, Lisbon, Portugal

² Laboratory for Chemical Technology, Ghent University, Ghent, Belgium

October 2022

Abstract

The study of aromatic admixture impact over *n*-alkane hydrocracking was achieved by following *n*-octane conversion, isomer selectivity, and catalyst deactivation at different conditions, over a proven well-balanced Pt/HUSY catalyst. With sufficiently high hydrogen-to-hydrocarbon ratio (80 - 200), no shift in hydrocracking regime was observed, as the introduction of toluene had no effect on catalyst stability, *n*-octane conversion, and isomer selectivity. Toluene was completely converted to hydrogenation products. Lowering hydrogen-to-hydrocarbon ratio (6.5) resulted in catalyst deactivation, which was stronger at lower applied pressure. Toluene conversion was not complete and products of bimolecular aromatic reactions on acid sites were detected. These products are coke precursors thus being considered responsible for catalyst deactivation. At higher temperatures, non-ideal hydrocracking was observed. Although further investigation could be done on this topic, hydrogen-to-hydrocarbon ratio appears to be the key parameter to control the effects of aromatic molecules on *n*-alkane hydrocracking.

Keywords: Hydrocracking, metal/acid site ratio, aromatic impact, catalyst activity.

1. Introduction

The hydrocracking process is very important for the oil refining industry, as it allows for the valorization of low value heavy oils (vacuum gas oil, bitumen) into high value middle distillates (jet fuel, kerosene). [1][2] In recent years, it has been studied the use of this process as a viable solution to produce biofuels, using cooking oils and mixtures of said oils and heavy oils. Despite carrying higher operational and capital costs, the increase in fuel prices and stricter environmental legislations favor the use of the hydrocracking process to reach higher yields of desired products while reducing the amount of residual fuel oil produced. Hydrocracking presents other benefits, namely being less prone to coking, being able to obtain better isomer yields and having a broad range of products that can be manipulated by altering the process conditions or the catalyst used[3][4] Hydrocracking industrial feeds are a complex mixture of alkanes, cycloalkanes, aromatics and other cyclic molecules.

Hydrocracking reaction occurs over a bifunctional catalyst with metal and acid sites, under hydrogen

atmosphere. Reaction mechanism is shown in Figure 1 [4]. The first step in the mechanism is the physical adsorption of the reactant to the catalyst surface, followed by dehydrogenation to unsaturated hydrocarbons on metal sites. These intermediate molecules are diffused onto Brønsted acid sites, where they are protonated, yielding alkyl-carbenium ions. The protonated species will undergo elementary reactions of isomerization (alkyl and hydride shifts, protonated-cyclopentane branching) and cracking (β -scission). The species will then be deprotonated, followed by hydrogenation on metal sites. Cycloalkanes follow a similar mechanism as linear alkanes but present different reaction network due to added isomerization reactions on the ring (intra-ring alkyl shifts, cyclic PCP branching), ring opening reactions (endocyclic β -scission) and dealkylation (exocyclic β -scission). Reaction rates decrease in order from alkyl-shifts to PCP branching to β -scission, which indicates that isomers are the primary products [4][5].

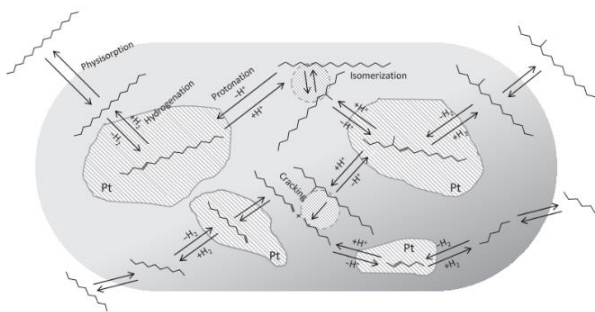


Figure 1: Bifunctional mechanism for the hydrocracking of *n*-hexadecane over Pt-loaded catalyst. [4]

Aromatic molecules possess special properties and stability when compared with other hydrocarbons due to their de-localized π -electrons clouds. Consequently, the hydrocracking reaction network of aromatic molecules is more extensive than the ones of alkanes and cycloalkanes, making it more complex to understand, since these molecules can react directly on both metal and acid sites, as shown in Figure 2. Aromatic compounds can be hydrogenated on metal sites, after which they will undergo the same elementary reaction reactions as the other saturated hydrocarbons. Alternatively, aromatic molecules can adsorb directly to the catalyst acid sites where they are protonated, yielding aromatic carbenium ions which will then undergo further reactions of isomerization (alkyl shifts, transalkylation) and cracking (dealkylation). [6]–[9]

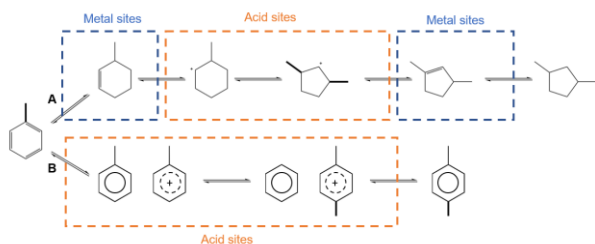


Figure 2: Possible toluene reaction schemes under low hydrogen-to-hydrocarbon ratio conditions.

The balance between metal and acid sites of a given catalyst is a key controlling parameter for the hydrocracking regime that is observed. Ideal hydrocracking is observed when the metal catalyzed reactions ((de)hydrogenation) are quasi-equilibrated while the reactions that occur on acid sites are rate-determining. [10]–[12] This prevents the occurrence of consecutive skeletal rearrangements/cracking reactions without intermediate protonation and hydrogenation (see Figure 1), resulting in maximal isomer yield. The equilibrium of (de)-hydrogenation reactions can be

achieved with sufficiently high metal to acid site ratio and is also dependent on process conditions and the distance between metal and Brønsted acid sites [10][13][14]. Decreasing metal site concentration or increasing acid site concentration will lead to a regime known as non-ideal hydrocracking, where both the metal and acid catalyzed reactions are kinetically relevant. In this situation, the (de)-hydrogenation step is slower, resulting in the occurrence of multiple consecutive reactions on a single acid site, consequently leading to higher yields of cracking products.

The observed hydrocracking regime not only is dependent on metal to acid site ratio of the catalyst, but also on the process conditions. Higher temperatures favor non-ideal hydrocracking given that both acid and metal catalyzed reaction rates increase in temperature however, the temperature dependence of acid catalyzed reactions is higher than metal catalyzed [10]. This means that an increase in temperature results in the need of higher metal concentration to ensure ideal hydrocracking. Higher total pressure induces a shift from non-ideal to ideal hydrocracking. An increase in total pressure leads to an increase in hydrogen partial pressure and, consequently, the (de)hydrogenation rate. In ideal hydrocracking, thermodynamics control the (de)hydrogenation reactions and due to Le Chatelier principle, the overall conversion will be decreased. This pressure dependence of *n*-alkane conversion is one of the biggest indicators for the occurrence of ideal hydrocracking.[10] Higher hydrogen-to-hydrocarbon ratio favors non-ideal hydrocracking. Lastly, the feedstock carbon number also impacts the hydrocracking regime, as alkanes with higher carbon number have larger reaction network, which increases the number of possible acid-catalyzed reactions, thus requiring higher concentration of metal sites. [10][14]

The admixture impact of aromatic molecules on *n*-alkane hydrocracking has not been systematically studied yet, however several investigations managed to identify certain trends related to this effect [2][15]–[18]. Generally, the introduction of aromatic molecules inhibits *n*-alkane conversion and can lead to a decrease in catalyst stability, depending on feed composition and catalyst used. These inhibitory effects can be related to the preferential adsorption of aromatic molecules on acid sites or diffusion limitations caused by the size of the aromatic compound inside the catalyst pores.

It is worth noting that the ability to modify reaction rates and selectivity, by co-feeding certain aromatic compounds, can be used on reactor operations and catalyst design.

The goals of this investigation are the experimental determination of aromatic component (toluene) impact on effective metal/acid site ratio for *n*-alkane (*n*-octane) hydrocracking over bifunctional catalyst (Pt/HUSY) at different operating conditions, while also assessing the influence of aromatic molecules on catalyst deactivation. The study of the impact hydrogen-to-hydrocarbon ratio will also be analyzed. This is achieved by following *n*-alkane conversion, isomer selectivity and catalyst activity under different conditions of pressure, temperature and space-times. Pt-HUSY catalyst was used as platinum presents great hydrogenation strength and the zeolite has sufficiently strong acid activity and due to its large pore size, prevents shape selectivity issues related to the presence of aromatic molecules.

2. Experimental Procedures

2.1 Catalyst Preparation

0.3 wt% Pt/HUSY catalyst was prepared in-house using the incipient wetness impregnation method, starting from HUSY zeolite (CBV712 with molar SiO₂/Al₂O₃ ratio of 12, from Zeolyst). Tetraammineplatinum(II)-nitrate hexahydrate [Pt(NH₃)₄(NO₃)₂·6H₂O (Sigma Aldrich (99,995% pure)) was used as precursor. The catalyst was left to mature overnight at room temperature after which it was dried in oven (Memmert) at a temperature of 110 °C for 10 hours. The catalyst was then calcined in a calcination oven (model P330 by Nabertherm) where it was heated using the rate of 5 °C/min and kept at 150°C, 250°C and 350°C for one hour and at 500 °C for two hours. The material was pelletized by applying 5 tons of pressure using a hydraulic press and was then sieved with a vibrating device (AS 200, by Retsch), to achieve the desired range of particle size (100 – 200 μm).

2.2 Catalyst Characterization

An insight in the physical and chemical properties is ensured by catalyst characterization, by using different characterization techniques.

Nitrogen adsorption-desorption was used to determine the pore structure and catalyst specific

surface area on a TriStar II device, at 77 K using the t-plot method.

Platinum content was investigated using inductively coupled plasma spectroscopy (ICP-OES), with IRIS Intrepid II XSP from Thermo Scientific.

Platinum reduction was analyzed using hydrogen temperature-programmed reduction (H₂-TPR) on Micrometics Autochem II 2920 device. Hydrogen-oxygen titration was used to determine the platinum dispersion and the average particle size, using the same device as H₂-TPR. The local structure of the zeolite, platinum dispersion and particle size were also investigated using transmission electron microscopy (TEM), in a JEM-2200FS Cs microscope device with Schottky type field emission gun and EDX.

The acidity of the catalyst was evaluated using ammonia temperature-programmed desorption (NH₃-TPD), using Micrometics AutoChem 2920 device.

2.3 Catalytic Studies

Hydrocracking reaction was investigated using the high-throughput setup designed by Zeton, present in the Laboratory for Chemical Technology (Ghent University) [19]. The continuous isothermal reactor (780 mm in length and internal diameter of 11 mm) is contained in a furnace which ensures temperature control. Hydrogen (reactant), nitrogen (inert) and methane (internal standard) are supplied for the experiments using thermal mass flow controllers (Bronkhorst) and their flows are set through LabView software and control computer. The liquid reactant feed is supplied from a flask using HPLC pump (Knauer Azura P4.1s) and the flow was controlled by monitoring the reactant flask weight on a regular basis. The catalyst bed was sieved to diameters between 100 – 200 μm and diluted using α-Al₂O₃ particles in a mass ratio of 1/3 (catalyst/inerts) to ensure no mass and heat transfer limitations. The catalyst was activated under pure hydrogen flow. Reactor pressure is controlled using a back-pressure regulator (Equilibar H3P High Pressure), containing a membrane and piloted by nitrogen flow. The setup is heat traced (200 °C) to prevent the condensation of the reactor effluent. The reaction products were analyzed using an online gas chromatograph (850 Series II, Agilent Technologies) equipped with a fire

ionization detector and a non-polar capillary column.

2.4 Definition of experimental space

For this experimental campaign, the selected model compounds for alkane and aromatic were *n*-octane and toluene, respectively. These molecules are representative of the paraffins and aromatic molecules present in oil fractions that are generally subject to hydrocracking. The reaction network of *n*-octane is extensive enough to efficiently observe transitions between ideal and non-ideal hydrocracking. *n*-octane and toluene have similar size and comparable physisorption enthalpies over USY zeolites [8][20][21], which reduces the effects of preferential physical adsorption to the zeolite.

The operating conditions were selected to ensure a broad range of *n*-octane conversion (10% - 55%) to have minimal experimental error and reliable comparison between kinetic measurements. The partial pressure of the model components was kept constant throughout the experiments (0.10 bar for *n*-octane and 0.025 bar for toluene). The experiments were conducted at two total pressures (10 and 20 bar) which allows identification of ideal hydrocracking regime. The temperatures used varied between 270 °C and 290 °C. The admixture effect of toluene was experimentally assessed by using 4:1 *n/n* mixture of *n*-octane and toluene. Hydrogen to hydrocarbon ratio changed throughout the experimental campaign to ensure constant partial pressure of model components but also to analyze its effect on *n*-octane hydrocracking, by following toluene hydrogenation products. The operating conditions used in the present investigation are summarized in Table 1.

3. Results

3.1 Catalyst Characterization

The results obtained from the catalyst characterization can be found in

Table 2 and show the physico-chemical properties of the synthesized 0.3 wt% Pt/HUSY.

Based on the results of nitrogen adsorption, porosity and surface area were similar to what has been previously reported [22]. Si/Al ratio was also found to be comparable to other investigations.[22]

NH₃-TPD shows that the addition of the zeolite did not impact the acidity of the zeolite. From ICP analysis, it was concluded that the elemental composition was similar to what was expected.

TEM identified larger particles than what was observed in previous investigations [22], which could be explained by the relatively low reduction degree obtained by H₂-TPR.

The metal dispersion of the catalyst and average particle size, obtained with H₂-O₂ titration, were found to be relatively poor, leading to the conclusion that these results were not reliable. The theoretical concentration of Brønsted acid sites was calculated using the values of Si/Al ratio obtained through ICP and was used to determine the metal-to-acid sites ratio of the catalyst considering the metal reduction.

Table 1: Experimental conditions used in the experimental campaign.

Catalyst	Feed composition (mol/mol)		Temperature (°C)	Pressure (bar)	Space time (kg s/mol)	H ₂ /HC ratio (mol/mol)	N ₂ /H ₂ ratio (mol/mol)	Partial Pressure (bar)	
	<i>n</i> -octane	toluene						<i>n</i> -octane	toluene
0.3 wt% Pt/HUSY	1	0	270 - 290	10 - 20	300 - 615	100 - 200	(no N ₂ was used)	0.10	0
	4	1	270 - 290	10 - 20	300 - 615	80 - 170	(no N ₂ was used)	0.10	0.025
	4	1	270 - 290	10 - 20	300 - 615	6.5	11.5 - 24	0.10	0.025

Table 2: Summary of the obtained results from catalyst characterization.

		0.3 wt% Pt/HUSY
Pt loading (wt%) - ICP		0.311
Pt reduction degree (wt%) – H ₂ TPR		36.5
Pt dispersion (%) – H ₂ -O ₂ titration		13.0
$n_P/n_{H^+} \times 10^3$ (mol/mol)		5.76
Acidity (mmol/g) – NH ₃ TPD		1.01
Specific surface area (m ² /g) - N ₂ adsorption t-plot		602
Average particle size (nm)	TEM	1.09

3.2 Catalytic studies

3.2.1 Pure *n*-octane feed

The first set of experiments was done with a pure *n*-octane feed to prove that the catalyst was well balanced at applied conditions. In this way a reliable comparison with experiments with toluene admixture is assured.

Figure 3 shows *n*-octane conversion obtained under different experimental conditions as a function of space time and it is possible to identify the trends which indicate ideal hydrocracking occurrence - such as a decrease of *n*-octane conversion for higher total pressure. Based on the results from the previous work by Korica et al [22], higher conversions were expected at applied conditions. The difference in conversion could be explained by the occurrence of preferential pathways in the catalytic bed, catalyst deactivation or poor catalyst loading. Despite of this, the catalyst can still be considered as well-balanced as conversion decreases with total pressure and *n*-octane isomer yield is comparable with previous investigations.

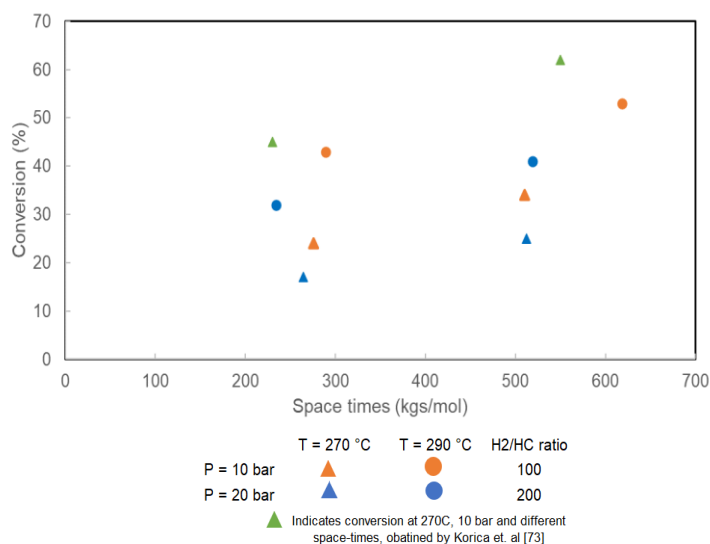


Figure 3: *n*-octane conversion, when fed pure at different temperatures and pressures, high hydrogen-to-hydrocarbon ratio, as a function of space time calculated based on *n*-octane flow over 0.3 wt% Pt/HUSY. Green triangles indicate results obtained in previous investigations by Korica et al. [22] used for comparison.

3.2.2 Experiments with the mixture of *n*-octane and toluene (4:1 *n/n*) and high H₂/HC ratio

The experiments with mixed feed of 4:1 *n/n* *n*-octane/toluene were carried out to assess the impact of toluene co-feed over *n*-octane hydrocracking. Partial pressures of *n*-octane and toluene were kept constant, by adjusting hydrogen-to-hydrocarbon ratio.

To evaluate the stability of the catalyst, time on stream (TOS) tests were done in parallel at different temperatures and space-times. Figure 4 shows that the catalyst remained active after the incorporation of toluene in the feed, given that the conversions remained constant for at least four hours of time on stream.

The *n*-octane conversion obtained at different operating conditions is shown in Figure 6. For most of the experimental points, no significant change in conversion was observed. However, there is one experimental point (T = 290 °C, P = 10 bar, ST = 288 Kgs/mol) that shows a considerable decrease in conversion when *n*-octane is fed pure compared to when it is fed in combination with toluene. Given the fact that this behavior is only noted for this single point, it can be considered as an outlier. No shift from ideal to nonideal hydrocracking is induced. This claim is validated by the *n*-octane isomer yield

shown in Figure 5, since it is maximal regardless of the feed composition.

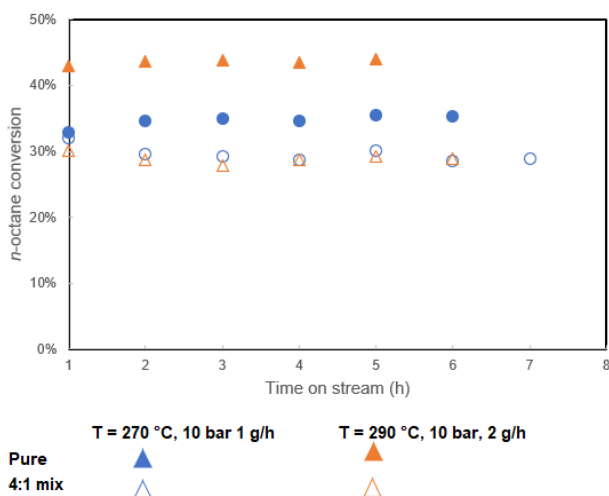


Figure 4: *n*-octane conversion, when fed pure or in a 4:1 *n/n* mixture with toluene and high hydrogen-to-hydrocarbon ratio, at (270 °C, 10 bar, 1 g/h), and (290 °C, 10 bar, 2 g/h), as function of time on stream.

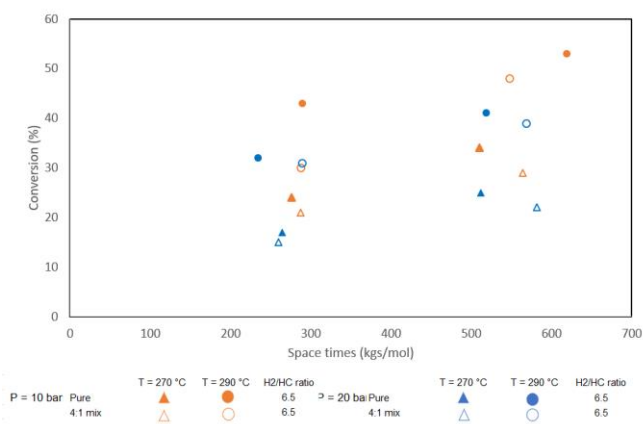


Figure 6: *n*-octane conversion, when fed pure (full symbols) or in a 4:1 *n/n* mixture with toluene and high hydrogen-to-hydrocarbon ratio, at different temperatures and pressures, as a function of space time calculated based on *n*-octane flow over 0.3 wt% Pt/HUSY

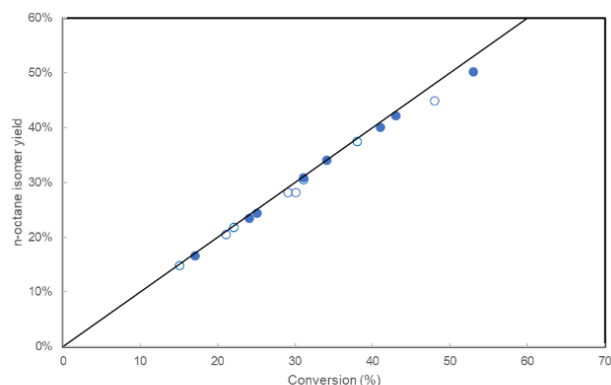


Figure 5: *n*-octane isomer yield, when fed pure (full symbols) or in a 4:1 *n/n* mixture with toluene and high hydrogen-to-hydrocarbon ratio, as a function of *n*-octane conversion.

3.2.3 Experiments with the mixture of *n*-octane and toluene (4:1 *n/n*) and low H_2/HC ratio

Given that toluene can either be hydrogenated into methylcyclohexane (further following classical hydrocracking mechanism) or react directly on acid sites through disproportionation or transalkylation reactions, the concentration of hydrogen will impact the rate of each reaction, which will have effects on the overall hydrocracking of *n*-octane. To study the impact of excess hydrogen, the hydrogen-to-hydrocarbon ratio was lowered to 6.5, with nitrogen being added as inert gas to keep the partial pressures of *n*-octane and toluene constant throughout all the experimental campaign. The results are shown in Figure 7.

Catalyst deactivation was observed across most experimental conditions. This effect was more pronounced at lower pressure as can be observed on Figure 7-(C) and Figure 7-(D). In these figures it is recognized that the conversion decrease at 10 bar is 30% (290 °C, 1 g/h) and 25% (290 °C, 2 g/h) while the drop in *n*-octane conversion at 20 bar is only around 10% in both cases. The deactivation also appears to be more pronounced when higher space times (lower liquid flow) are employed. It is also possible to detect a shift to non-ideal hydrocracking when the temperature is 290 °C, given that the conversions obtained for pressure of 20 bar are higher than the *n*-octane conversions reached when the pressure is lower. The intensity of catalyst deactivation also appears to be related to total pressure. It is observed that higher pressure (more inert gas) leads to less deactivation of the catalyst, likely due to avoiding bimolecular reactions of toluene on acid sites which lead to coke formation.

The *n*-octane isomer yield was also studied when the hydrogen-to-hydrocarbon was lowered to 6.5 and is shown on the Figure 8. The characteristic isomer yield of ideal hydrocracking is respected at lower conversions (10% - 20%) however, deviation from this ideal behavior is observed at higher *n*-octane conversions (24% - 42%) which indicates a

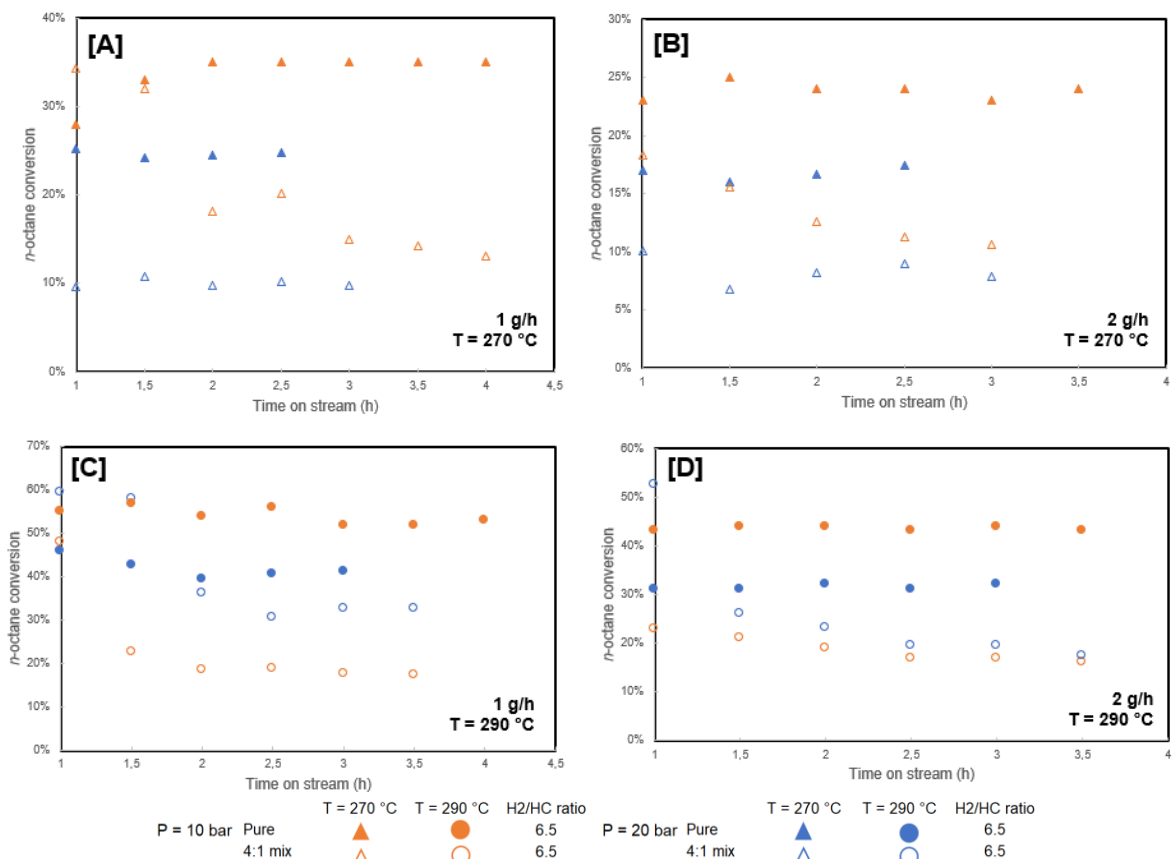


Figure 7: *n*-octane conversion, when fed pure (full symbols) or in a 4:1 *n/n* mixture with toluene and hydrogen-to-hydrocarbon ratio of 6.5, at different temperatures and pressures, as function of time on stream.

shift to non-ideal behavior. These experimental points were all taken at 290°C, which verifies that at this temperature ideal hydrocracking is no longer occurring, as referred previously. As consequence of this transition in hydrocracking regime, more *n*-octane cracking products are detected at higher temperature.

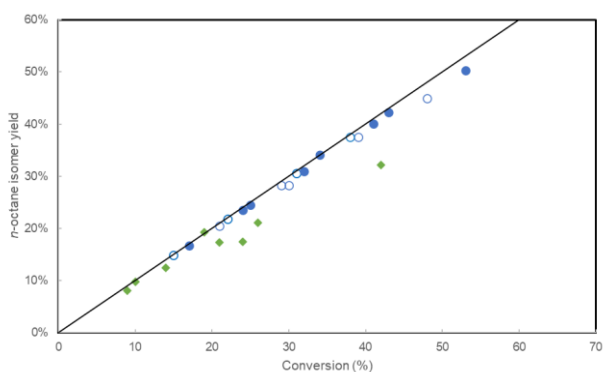


Figure 8: *n*-octane isomer yield, when fed pure (full symbols); in a 4:1 *n/n* mixture with toluene and high hydrogen-to-hydrocarbon ratio (blue circles) or in a 4:1 *n/n* mixture with toluene and hydrogen-to-hydrocarbon ratio of 6.5 (green diamonds), as a function of *n*-octane conversion.

The conversion and product selectivity of the toluene were also analyzed, shown in Figure 9 and Figure 10. It can be observed that at high hydrogen-to-hydrocarbon ratio toluene conversion is 100% as only methylcyclohexane (and its isomers) were detected, which is line with the fact that no deactivation was observed in these experiments. However, with lower hydrogen-to-hydrocarbon, the conversion of toluene decreased and although methylcyclohexane was still the major product of toluene, a small percentage (7%) of it was converted into benzene and xylene through acid catalyzed reactions which occupy the acid sites and lead to the subsequent deactivation of the catalyst. From Figure 10 is possible to observe that for the reactions that are not in thermodynamic equilibrium, lower space times result in decreased toluene conversion. However, at temperature of 290 °C higher pressure leads to an increase in toluene conversion.

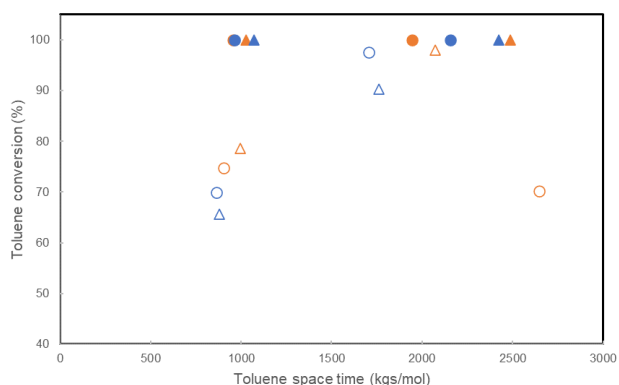


Figure 9: Toluene conversion, when fed with high hydrogen-to-hydrocarbon ratio (full symbols) or hydrogen-to-hydrocarbon ratio of 6.5, at different temperatures and pressures, as function of space time calculated based on toluene flow over 0.3 wt% Pt/HUSY.

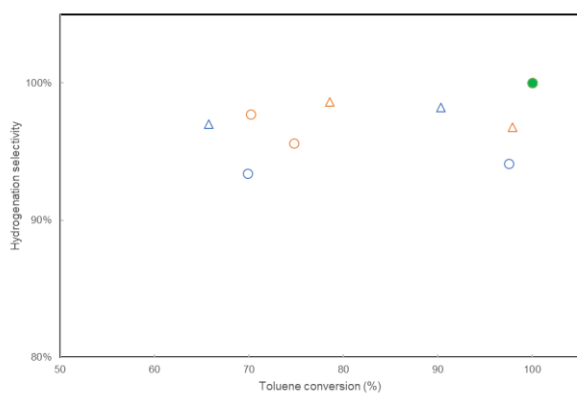


Figure 10: Toluene selectivity to hydrogenation products, when fed with high hydrogen-to-hydrocarbon ratio (green) or hydrogen-to-hydrocarbon ratio of 6.5, at different temperatures and pressures, as function of toluene conversion.

4. Discussion

The impact of toluene admixture on *n*-octane hydrocracking is summarized by comparing *n*-octane conversion and isomer yield, across different experimental conditions.

With high hydrogen-to-hydrocarbon ratio, no deactivation or decrease in *n*-octane conversion was observed. Toluene was completely hydrogenated to methylcyclohexane, which followed further bifunctional mechanism represented in Figure 2-(A). No acid catalyzed reactions of toluene occurred. Given the fact that at these conditions no catalyst deactivation was detected, acid catalyzed reactions of toluene can be considered as the cause catalyst deactivation. Despite the preferential physisorption of the aromatic molecules onto the catalyst and complete toluene hydrogenation, the catalyst remained well balanced for *n*-octane conversion, indicating that the introduction of toluene was not enough to

impact the metal-to-acid site ratio needed to ensure ideal hydrocracking.

Alternatively, when low hydrogen-to-hydrocarbon ratio was employed, the catalyst was rapidly deactivated, likely due to preferential toluene adsorption on acid sites. This effect was stronger at lower applied pressure. Toluene conversion was not complete under these conditions and the selectivity towards hydrogenation products was lower, however it remained relatively high. Part of the converted toluene reacted directly on the acid sites of the catalyst (see Figure 2-(B)) through transalkylation and disproportionation reactions yielding benzene and xylenes. These reactions significantly decrease the availability of acid active sites for the isomerization/cracking reactions of *n*-octane leading to the poisoning the catalyst and its deactivation. The results obtained are in line with what has been previously reported in literature.

A transition from ideal to non-ideal hydrocracking was noticed at 290 °C (see Figure 7-(C) and Figure 7-(D)) since higher pressure resulted in higher conversion and was confirmed by lower *n*-octane isomer selectivity. This can be related to both the introduction of toluene and the change in operating conditions. At lower temperature, toluene hydrogenation reduces the amount of available metal sites which could induce a shift towards non-ideal hydrocracking. However, since toluene also reacts on acid sides their availability is also decreased, resulting that the overall ratio of available metal and acid sites is still high enough to ensure ideal hydrocracking. At the temperature of 290 °C, toluene continues to react on both metal and acid sites however, coupled with the effects of increasing temperature and pressure, the ratio of concentrations of available metal and acid ratio is lowered to the point where non-ideal hydrocracking occurs.

It was observed that higher pressure led to less pronounced deactivation of the catalyst (see Figure 7-(C) and Figure 7-(D)). The partial pressures of toluene and *n*-octane were kept constant across all experiments meaning that a change in total pressure only altered the partial pressure of inert gas (nitrogen). The deactivation of catalyst occurs due to coke formation which is formed in bimolecular acid catalyzed reactions of toluene. Higher amount of nitrogen, which is present at higher total pressure, results in less frequent

molecular collisions. This effect is assumed to be a reason for better stability of the catalyst at higher total pressure.

The addition of toluene showed that the main impact of this molecule occurred on the catalyst acid sites, which leads to deactivation and lower *n*-octane conversion.

It can be deduced that high excess of hydrogen will favor toluene hydrogenation, shifting the equilibrium of this reaction towards the products, and suppressing bimolecular aromatic reactions on acid sites, which leads to deactivation.

5. Conclusions

The present work allowed for an insightful understanding of the effects of the addition of aromatic components on alkane hydrocracking by studying *n*-octane and toluene as model molecules.

The synthesized catalyst was characterized with different techniques which allowed for a better understanding of its physico-chemical properties. The addition of platinum did not affect the acidity of the catalyst. The catalyst elemental composition, zeolite surface area and porosity were in accordance with what was expected and with what had been previously reported.

It was found that the addition of toluene to the alkane hydrocracking feed had no impact on the conversion of *n*-octane and on the occurrence of ideal hydrocracking when high hydrogen-to-hydrocarbon ratio was used. The catalyst stability was also not affected by the introduction of the aromatic molecule in the feed. When the hydrogen partial pressure was reduced, by addition of nitrogen as diluent, catalyst deactivation was observed across all experimental conditions. The deactivation was more noticeable at lower applied pressure. It was also noticed a transition to non-ideal hydrocracking, at the temperature of 290 °C, as an increase in pressure lead to an increase in conversion.

It was found that toluene conversion and selectivity is dependent on hydrogen-to-hydrocarbon ratio. With high excess hydrogen, toluene conversion is complete and the selectivity towards hydrogenation products is 100%. When hydrogen-to-hydrocarbon ratio is lower, not all toluene is converted and small

selectivity towards acid catalyzed products is detected. Despite hydrogenation products still being more prevalent on the reactor effluent, catalyst deactivation was observed. This indicates that bimolecular aromatic reactions on acid sites are responsible for the deactivation of the catalyst. The impact of toluene on *n*-octane hydrocracking can be minimized with high hydrogen excess since it promotes the hydrogenation reaction of toluene molecules.

References

- [1] L. C. Castañeda, J. A. D. Muñoz, and J. Ancheyta, "Combined process schemes for upgrading of heavy petroleum" in *Fuel*, 2012, vol. 100, pp. 110–127. doi: 10.1016/j.fuel.2012.02.022.
- [2] M. Busto, J. M. Grau, J. H. Sepulveda, O. M. Tsendra, and C. R. Vera, "Hydrocracking of long paraffins over Pt-Pd/WO₃-ZrO₂ in the presence of sulfur and aromatic impurities" *Energy and Fuels*, vol. 27, no. 11, pp. 6962–6972, 2013. doi: 10.1021/ef401138v.
- [3] Corrosionpedia, "Hydrocracking" 2018. <https://www.corrosionpedia.com/definition/1675/hydrocracking-petroleum-processing> (accessed Mar. 24, 2022).
- [4] J. W. Thybaut and G. B. Marin, "Multiscale Aspects in Hydrocracking: From Reaction Mechanism Over Catalysts to Kinetics and Industrial Application" in *Advances in Catalysis*, vol. 59, Academic Press Inc., 2016, pp. 109–238. doi: 10.1016/bs.acat.2016.10.001.
- [5] G. G. Martens, J. W. Thybaut, and G. B. Marin, "Single-event rate parameters for the hydrocracking of cycloalkanes on Pt/US-Y zeolites" *Ind Eng Chem Res*, vol. 40, no. 8, pp. 1832–1844, 2001. doi: 10.1021/ie000799n.
- [6] S. S. Arora and A. Bhan, "Kinetics of aromatics hydrogenation on HBEA" *J Catal*, vol. 383, pp. 24–32, 2020. doi: 10.1016/j.jcat.2019.12.039.
- [7] P. Castaño, J. M. Arandes, B. Pawelec, M. Olazar, and J. Bilbao, "Kinetic modeling for assessing the product distribution in toluene hydrocracking on a Pt/HZSM-5 catalyst," *Ind Eng Chem Res*, vol. 47, no. 4, pp. 1043–1045, 2008. doi: 10.1021/ie071154r.

- [8] K. Toch, J. W. Thybaut, B. D. Vandegheuchte, C. S. L. Narasimhan, L. Domokos, and G. B. Marin, "A Single-Event MicroKinetic model for 'ethylbenzene dealkylation/xylene isomerization' on Pt/H-ZSM-5 zeolite catalyst," *Appl Catal A Gen*, vol. 425–426, pp. 130–144, 2012. doi: 10.1016/j.apcata.2012.03.011.
- [9] J. M. Silva Ribeiro, F. Ram, and R. E. Benazzi M Guisnet, "Transformation of an ethylbenzene-o-xylene mixture on HMOR and Pt-HMOR catalysts. Comparison with ZSM-5 catalysts" 1995. doi: [https://doi.org/10.1016/0926-860X\(94\)00259-2](https://doi.org/10.1016/0926-860X(94)00259-2).
- [10] J. W. Thybaut *et al.*, "Acid-metal balance of a hydrocracking catalyst: Ideal versus nonideal behavior" *Ind Eng Chem Res*, vol. 44, no. 14, pp. 5159–5169, 2005. doi: 10.1021/ie049375.
- [11] G. G. Martens, G. B. Marin, J. A. Martens, P. A. Jacobs, and G. v. Baron, "A Fundamental Kinetic Model for Hydrocracking of C8 to C12 Alkanes on Pt/US-Y Zeolites" *J Catal*, vol. 195, no. 2, pp. 253–267, 2000. doi: 10.1006/jcat.2000.2993.
- [12] J. Weitkamp, "Catalytic Hydrocracking-Mechanisms and Versatility of the Process" *ChemCatChem*, vol. 4, no. 3, pp. 292–306, 2012. doi: 10.1002/cctc.201100315.
- [13] T. F. Degnan and C. R. Kennedy, "Impact of catalyst acid/metal balance in hydroisomerization of normal paraffins" *AIChE Journal*, vol. 39, no. 4, pp. 607–614, 1993. doi: 10.1002/aic.690390409.
- [14] N. Korica, P. S. F. Mendes, J. de Clercq, and J. W. Thybaut, "Interplay of Metal-Acid Balance and Methylcyclohexane Admixture Effect on n-Octane Hydroconversion over Pt/HUSY" *Ind Eng Chem Res*, vol. 60, no. 34, pp. 12505–12520, 2021. doi: 10.1021/acs.iecr.1c01775.
- [15] M. Guisnet and V. Fouche, "Isomerization of n-hexane on platinum dealuminated mordenite catalysts III. Influence of hydrocarbon impurities" *Applied Catalysis*, vol. 71, no. 2, pp. 307-317, 1991. doi: [https://doi.org/10.1016/0166-9834\(91\)85088-D](https://doi.org/10.1016/0166-9834(91)85088-D).
- [16] P. Sánchez, F. Dorado, M. J. Ramos, R. Romero, V. Jiménez, and J. L. Valverde, "Hydroisomerization of C6-C8 n-alkanes, cyclohexane and benzene over palladium and platinum beta catalysts agglomerated with bentonite" *Appl Catal A Gen*, vol. 314, no. 2, pp. 248–255, 2006. doi: 10.1016/j.apcata.2006.08.025.
- [17] J.-K. Chen, A. M. Martin, and V. T. John', "A kinetic analysis of competitive reaction in intrazeolitic media" *Chemical Engineering Science*, vol. 45 no. 3, pp. 575-586, 1990. doi: [https://doi.org/10.1016/0009-2509\(90\)87002-A](https://doi.org/10.1016/0009-2509(90)87002-A).
- [18] J. K. Chen, A. Martin, and V. John, "Modifications of n-Hexane Hydroisomerization over Pt/Mordenite as Induced by Aromatic Cofeeds" *Journal of Catalysts*, vol. III, pp. 425–428, 1998. doi: [https://doi.org/10.1016/0021-9517\(88\)90102-9](https://doi.org/10.1016/0021-9517(88)90102-9).
- [19] J. de Waele, T. Rajkhowa, and K. Toch, "High-Throughput Kinetic Setup (HTK-1): Manual and safety guidelines." 2015. [Online]. Available: www.lct.ugent.be
- [20] J. E. Denayer and G. v Baron, "Adsorption of Normal and Branched Paraffins in Faujasite Zeolites NaY, HY, Pt/NaY and USY" *Adsorption*, vol. 3, pp. 251-265, 1996. doi: <https://doi.org/10.1007/BF01653628>.
- [21] L. Xu, Y. Li, J. Zhu, and Z. Liu, "Removal of Toluene by Adsorption/Desorption Using Ultra-stable Y Zeolite" *Transactions of Tianjin University*, vol. 25, no. 4, pp. 312–321, 2019. doi: 10.1007/s12209-019-00186-y.
- [22] N. Korica *et al.*, "Mixture effects in alkane/cycloalkane hydroconversion over Pt/HUSY: Carbon number impact," *Fuel*, vol. 318, 2022. doi: 10.1016/j.fuel.2022.123651.